


Article

Experimental Research on the Performance Characteristics of Grouting Slurry in a High-Ground-Temperature Environment

Yangkang Yang ¹, Jiandong Niu ^{1,*} , Yong Sun ¹, Jianxin Liu ² and Liangliang Qiu ³

¹ School of Civil Engineering, Central South University, Changsha 410075, China; 214811093@csu.edu.cn (Y.Y.); jlinccc@163.com (Y.S.)

² College of Foreign Affairs, Central South University of Forestry and Technology, Changsha 410004, China; 13479546635@163.com

³ Changsha Hengde Geotechnical Engineering Technology Co., Ltd., Changsha 410075, China; klsh1019@163.com

* Correspondence: niudong@csu.edu.cn; Tel.: +86-152-731-379-96

Abstract: Grouting materials with good thermal insulation and reinforcement properties are the key factors in solving the temperature control problems of high geothermal tunnels using curtain grouting, as the existing grouting materials are unable to take into account the working performance and thermal insulation properties of high-temperature environments. In view of the above problems, this paper configures a high geothermal tunnel red-mud-based grouting material (RMGS) using red mud, carries out tests on the working performance (viscosity, setting time, and compressive strength) and thermal insulation performance (thermal conductivity and specific heat capacity) of the grouting materials at different temperatures (20, 40, 60, and 80 °C), and analyses the variation rules and micro-mechanisms of the various properties at different temperatures. The results show that the increase in temperature will accelerate the viscosity development and condensation of the grouting material and will also lead to the acceleration of the attenuation of the thermal conductivity of the three types of grouting material and the reduction in specific heat capacity. In addition, the appropriate temperature can improve the compressive strength of the material. The increase in temperature will accelerate the hydration reaction speed of the grouting material and will also lead to the development of the internal pore space of the material, which affects the macroscopic properties of the material and is the reason for the effect of the temperature on the performance of the grouting material. In terms of application, the cement slurry is suitable for grouting in a static water environment, the cement–water glass bi-liquid slurry is suitable for grouting in a dynamic water environment, and the RMGS is suitable for grouting in a high-ground-temperature environment.

Keywords: high-temperature tunnel; red mud; grouting materials; thermal insulation performance; viscosity



Citation: Yang, Y.; Niu, J.; Sun, Y.; Liu, J.; Qiu, L. Experimental Research on the Performance Characteristics of Grouting Slurry in a High-Ground-Temperature Environment. *Buildings* **2023**, *13*, 3005. <https://doi.org/10.3390/buildings13123005>

Academic Editor: Geo Paul

Received: 2 November 2023

Revised: 22 November 2023

Accepted: 28 November 2023

Published: 1 December 2023



Copyright: © 2023 by the authors. Licensee MDPI, Basel, Switzerland. This article is an open access article distributed under the terms and conditions of the Creative Commons Attribution (CC BY) license (<https://creativecommons.org/licenses/by/4.0/>).

1. Introduction

Tunnel construction faces many problems regarding high-ground-temperature tunnels [1–4], as they can deteriorate the construction operating environment and lead to a significant increase in operating costs [5–7]. Curtain grouting technology is one of the important methods to achieve temperature control in high-ground-temperature tunnels [8]. In response to the temperature control problems of high geothermal tunnels, some scholars [9] have explored methods of solving the problems of high geothermal environments at the technical level, but these methods have insufficient economic benefits and limited application conditions. While curtain grouting is one of the most effective methods to achieve temperature control in high geothermal environments [10], grouting materials with good thermal insulation properties are the key factors in achieving curtain grouting, so it is necessary to study grouting materials with good thermal insulation properties.

Studies have shown that cementitious grouting material has insufficient bonding at the pulp–rock interface at temperatures above 50 °C, and the strength of the material shows a reduction phenomenon [11,12]. The compressive strength of the cement stone in the material increases and then decreases with the increase in temperature, and the corresponding porosity and permeability increase [13]. The temperature has a significant effect on the relative peak stresses of the cement paste [14], which are achieved through an increase in the paste’s elasticity, plasticity, and viscosity, thereby increasing its yield stress [15]. Some scholars believe that temperature accelerates the hydration reaction of cement, and shrinkage occurs after the paste hardens in dry environments, which leads to cracks in interstitial defects and a decrease in workability [16–18].

Scholars have tried to add different admixtures and additives to the grouting materials as a way to enhance the performance of grouting materials in high-temperature environments. The joint action of fly ash and silica fume can ensure the rapid hardening of the grouting materials and enhance their early strength as well as long-term strength [19]. The volcanic ash activity in mineral admixtures can also improve the high-temperature working performance of concrete [16]. Fibre materials, especially steel fibres, are able to effectively inhibit the shrinkage phenomenon after hardening of the paste [17], and wavy steel fibres have the best effect on the improvement of compressive strength [20]. The addition of a quick-setting agent can improve the late strength of fly ash cement paste [21]; in addition, adding slag powder to the cement paste improves the fluidity and stability of the cement paste, and the late compressive strength is significantly improved [22].

In summary, it can be seen that the grouting in high geothermal tunnels is still dominated by common cement and cement–water glass, while the weak dispersion resistance of cement makes it difficult to effectively resist the scouring of high-temperature hot water, which leads to a poor plugging effect and poor economic benefits and is prone to ground-water contamination. In addition, the cement–water glass has too short a condensation time in high-temperature environments, which means it is prone to pipe plugging and has difficulty forming a sufficient thickness of the curtain circle layer.

Scholars have conducted extensive research on the influence of common materials on the performance of grouting materials, and a number of scholars have summed up the experience of their predecessors and configured a number of new grouting materials suitable for special geological environments. However, there are certain differences in the performance requirements of grouting materials in different geological environments, resulting in the specificity of these grouting materials, which can only be used for certain working conditions. Therefore, although there are many kinds of grouting materials on the market, the materials suitable for grouting in high-temperature tunnels are very rare. Red-mud-based grouting materials, which are configured by replacing part of the cement with red mud, have excellent working performance [23]. However, there are few engineering applications of red mud as a grouting material, there are few studies on its properties in high-temperature environments, and there is still a gap in the field of grouting reinforcement in high-temperature tunnels.

In view of this, this paper carries out the working performance and thermal insulation performance tests of a red-mud-based grouting material (RMGS), cement slurry, and cement–water glass bi-liquid slurry at different temperatures, analyses the law and degree of the influence of temperature on the basic performance of grouting materials and their microscopic mechanisms, and, on the basis of which, researches three kinds of grouting materials and their applicability in different environments. This test can provide a basis for the realization of temperature control of high geothermal tunnels, which is of great significance to the construction, maintenance, and repair of high geothermal tunnels and has value for engineering applications.

2. Materials and Methods

2.1. Materials

The red mud used in the test was selected from the Bayer red mud produced by Guangxi Pingguo Aluminium Industry, with a particle size of 0.005–0.075 mm and a density of 2.75 g/cm³. Red mud is a waste product of bauxite extraction from alumina industrial production and is known as red mud because of its high content of Fe₂O₃ and because its appearance is similar to that of the red-coloured mud; some red mud is brown due to the low content of Fe₂O₃, instead containing a large amount of CaO [23,24]. Red mud is a highly alkaline solid waste, usually with a pH > 11.0, which is polluting and is pretreated before use. Pretreatment includes (1) water washing to a pH of 8.0–8.5, (2) boiling and washing using acid, and (3) alkali precipitation after acid dissolution.

The cement used in this study is P.O 42.5 (ordinary silicate cement), produced in southern Hunan province, with a fineness of 800 mesh and a density of 3.05 g/cm³, which is in line with general Portland cement standards [25]. The quartz powder used is a powdered solid of pure quartz processed after a series of industrial procedures, with a fineness of about 160 mesh. The main component of the modifier is Na₂SiO₃ with a Baume degree of 25 and a modulus of 3.5. The chemical composition of the raw materials is shown in Table 1.

Table 1. Chemical composition of materials.

Compositions	CaO	Fe ₂ O ₃	SiO ₂	Al ₂ O ₃	SO ₃	Loss
Cement	60.1	4.13	25.11	6.72	2.01	1.93
Red mud	5.95	36.96	9.14	19.74	0.28	17.67
Quartz powder	0.05	0.23	99.2	0.35	0.01	0.16

2.2. Sample Preparation

RMGS was used as the test group, and its ratio composition is shown in Table 2. An ordinary cement slurry and a cement–sodium silicate slurry were used as the control group.

Table 2. Composition of the RMGS.

Compositions	Cement	Red Mud	Quartz Powder	Water	Modified Additives
Content	The amount of cement needed for the experiment	150% of the quality of cement	150% of the quality of cement	Water:Solid = 0.61:1	60% of the quality of cement

The water–cement ratio of the ordinary cement slurry was 0.6.

The cement–sodium silicate slurry had a water–cement ratio of 0.6, and the water glass admixture was 20% of the mass of cement [26].

The main component of water glass is Na₂SiO₃, with a Baume degree of 25 and a modulus of 3.5.

The physical properties of the RMGS after final setting are shown in Table 3.

Table 3. Table of physical properties of RMGS.

Temperature/°C	Density/(g·cm ³)	Porosity/%	Stone Rate/%	Bleeding Rate/%
20	1.62	18.51	96.8	3.2
40	1.68	18.72	97.2	2.8
60	1.71	18.98	97.5	2.5
80	1.76	19.39	98.7	1.3

Sample Preparation Procedure:

- (1) Dry ingredients were mixed according to the proportions in Table 2 and placed in a sealed container. The container was then positioned inside a constant-temperature water bath, with temperatures set at 20 °C, 40 °C, 60 °C, and 80 °C, and heated for 24 h, as shown in Figure 1a.
- (2) Isothermal water and the modifying agent were added to a mixing tank, followed by the preheated dry mixture. The mixing device was activated.
- (3) The viscosity of the resulting slurry was measured.
- (4) The specimens were subjected to curing in a constant-temperature water bath for the specified duration, followed by testing for various parameters, as shown in Figure 1b. The finished sample is shown in Figure 1c.

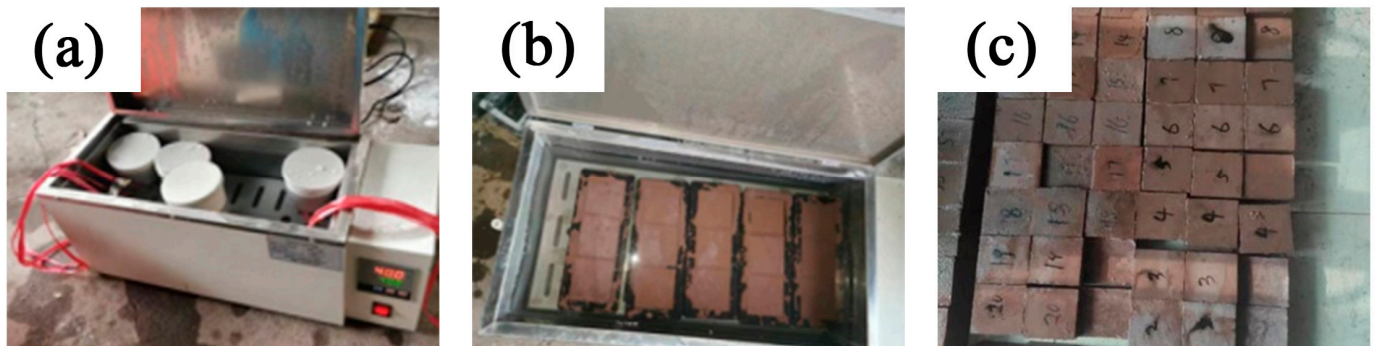


Figure 1. Sample preparation: (a) material preheating; (b) water bath heating; (c) finished test specimens.

2.3. Methods

Viscosity testing was conducted using a rotational viscometer, and the setting time was determined using the Vicat apparatus. Compressive strength was assessed through unconfined compressive strength tests, with test specimens measuring 70.7 mm × 70.7 mm × 70.7 mm, as illustrated in Figure 2.

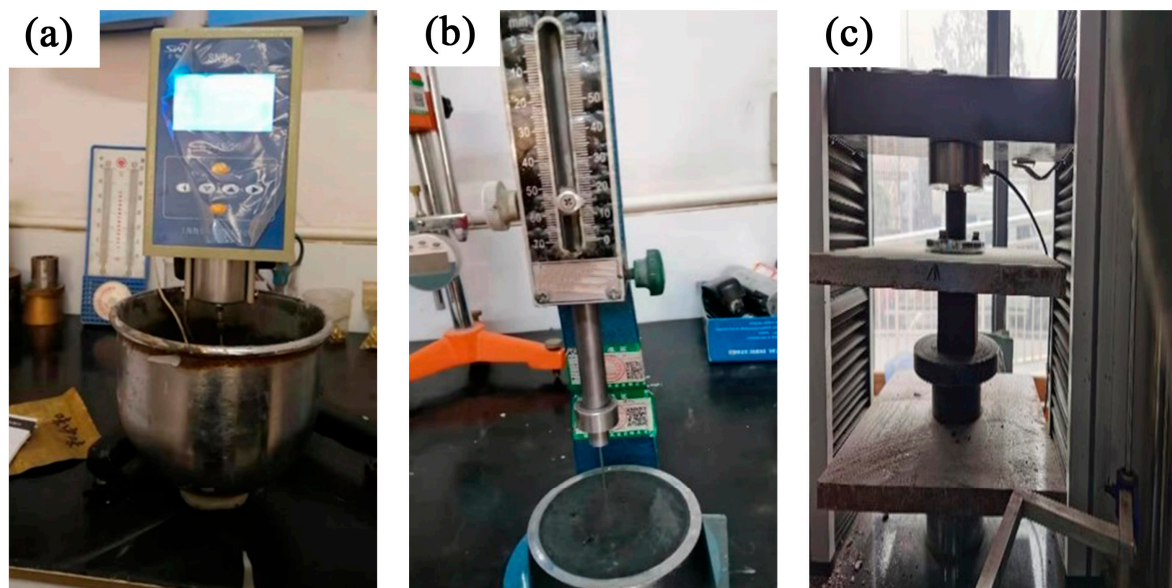


Figure 2. Laboratory experiments on grouting materials: (a) viscosity testing; (b) setting time testing; (c) compressive strength testing.

Thermal conductivity was assessed using triple-layer specimens measuring 40 mm × 40 mm × 160 mm. These specimens were placed in a water bath at the corresponding temperature for three days of curing before measurement. Thermal conductivity was determined using the guarded heat plate method [27], as depicted in Figure 3. Specific heat capacity determination employed the method of mixtures [28], as illustrated in Figure 4.

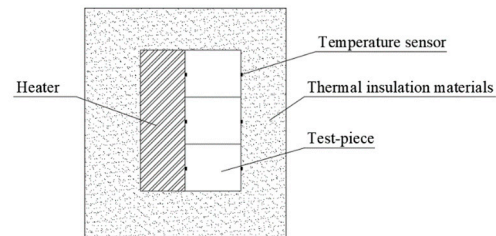


Figure 3. Thermal conductivity testing device.

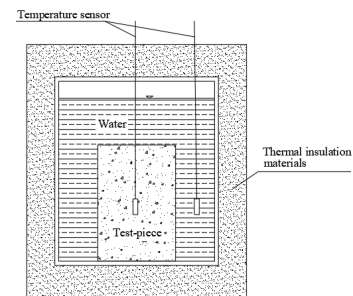


Figure 4. Specific heat capacity testing device.

Microscopic analysis was conducted using the F200X field-emission transmission electron microscope available at the Advanced Research Center of Central South University, as depicted in Figure 5. This instrument features intelligent scanning engines, a four-channel merging technique based on multiple STEM detectors, and differential phase contrast (DPC/iDPC) imaging technology. In TEM mode, it achieves a point resolution of 0.25 nm, while in STEM mode, the resolution is further enhanced to 0.16 nm.



Figure 5. F200X field-emission transmission electron microscope (HITACHI, Tokyo, Japan).

3. Results and Analyses

3.1. Viscosity

Viscosity reflects the internal resistance of the slurry flow and reflects the fluidity of the slurry as well as the resistance to scouring. The viscosity data of the cement slurry, cement–sodium silicate slurry, and RMGS at 20, 40, 60, and 80 °C were obtained through viscosity measurement tests under different temperature conditions, and the change curves of the three kinds of slurries' viscosity versus time under different temperature conditions are shown in Figure 6.

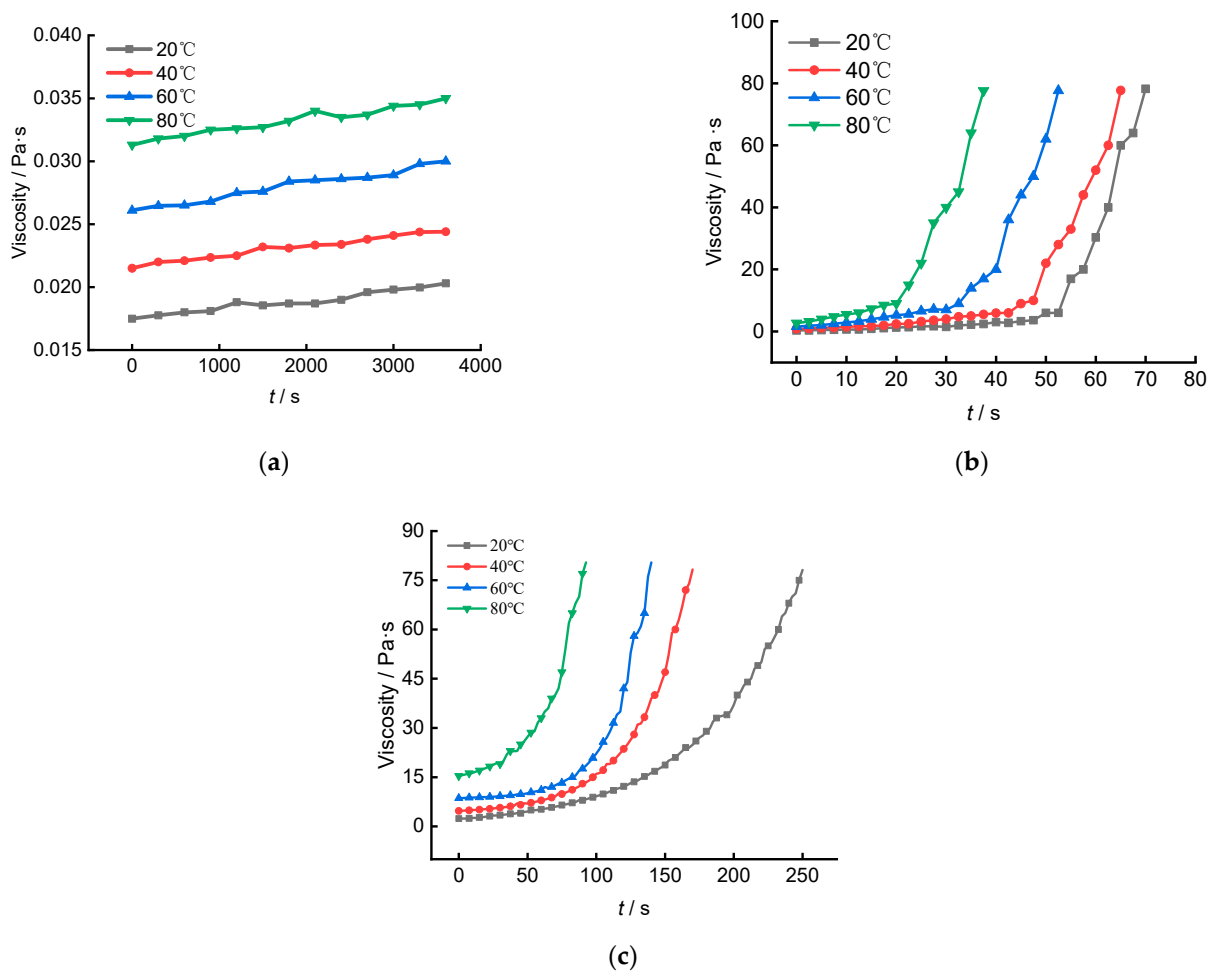


Figure 6. Viscosity–time relationship curve of grouting material at different temperatures: (a) cement slurry; (b) cement–sodium silicate slurry; (c) RMGS.

As can be seen from Figure 6, the higher the temperature, the higher the viscosity of the slurry, but the temperature does not change the trend of slurry viscosity change. Based on the effect of temperature on viscosity, the literature [26] gives the viscosity time-varying curve fitting equations for the cement slurry and cement–sodium silicate slurry. In this paper, the viscosity data of RMGS are fitted, and the fitting equations are shown in Table 4.

Table 4. Time-dependent viscosity equations for the RMGS at different temperature conditions.

Temperature (°C)	The Time-Varying Characteristic Equations of Viscosity	R ²
20	$\mu = 2.243e^{t/70.525} + 0.134$	0.999
40	$\mu = 0.797e^{t/37.268} + 3.934$	0.998
60	$\mu = 0.244e^{t/24.512} + 8.252$	0.995
80	$\mu = 1.906e^{t/25.676} + 13.557$	0.992

Note: μ is the viscosity, t is the time, and R² is the correlation coefficient.

According to the fitting results, the following conclusions can be obtained:

- (1) The viscosity time-varying equation obtained by the function fitting can effectively reflect the time-varying characteristics of the slurries, which can be applied to the calculation and simulation of grouting reinforcement in high-ground-temperature tunnels.
- (2) At the same temperature, the viscosity time-varying curves of the cement slurry, cement–sodium silicate slurry, and RMGS have large differences: the viscosity time-

varying curve of the cement slurry conforms to the linear function; the viscosity time-varying curve of the cement–sodium silicate slurry conforms to the power function; and the viscosity time-varying curve of the RMGS conforms to the exponential function.

- (3) The effect of temperature on the three slurries is similar, i.e., an increase in temperature accelerates the development of slurry viscosity and increases the viscosity value but does not affect the time-varying characteristics of the slurries.

The increase in temperature makes the ions involved in the hydration reaction more active, so it accelerates the hydration process of the grouting material; therefore, the higher the temperature, the faster the viscosity growth rate and the greater the viscosity. The main reason for the slow growth of viscosity in the early stage of the RMGS is that, under the action of a modifier, the silica-aluminium component in red mud undergoes a depolymerization reaction, the content of free water decreases, $[\text{SiO}_4]^{4-}$ and $[\text{AlO}_4]^{3-}$ undergo a polymerization reaction, and the free water consumed by the depolymerization reaction of the silica-aluminium component is roughly balanced with the free water generated by the new polymerization reaction. In the later stage, the viscosity of the slurry of the RMGS increases significantly because the hydration products in the slurry are generated in large quantities, and the slurry starts to harden [29], so the viscosity increases significantly; in addition, Na_2SiO_3 reduces the solubility of the hydration products and reduces the effect of the pores on the viscosity of the slurry, and the $[\text{SiO}_4]^{4-}$ combines with the Ca^{2+} in the cement to form a $\text{Ca}_5\text{Si}_6\text{O}_{16}(\text{OH})\cdot 4\text{H}_2\text{O}$ (C-S-H) gel that accelerates the hardening of the slurry. Therefore, due to the lack of excitation of the modifier in the cement monohydrate slurry, its viscosity grows slowly, and there is a big gap between the RMGS and the cement–sodium silicate slurry.

3.2. Setting Time

The setting time reflects the hardening characteristics of the slurry and the time of strength generation. Through the setting time test, the data of the initial and final setting time of the cement slurry, cement–sodium silicate slurry, and RMGS at 20, 40, 60, and 80 °C were obtained, and the change curves of the initial and final setting time of the three kinds of slurries with the temperature are shown in Table 5.

Table 5. Grouting material setting schedule.

Test Materials	Initial Setting Time/min				Final Setting Time/min			
	20 °C	40 °C	60 °C	80 °C	20 °C	40 °C	60 °C	80 °C
Cement Slurry	402	318	154	83	460	353	182	128
Cement–Sodium Silicate Slurry	31	18	12	10	52	48	42	27
The RMGS	325	140	74	34	434	265	191	135

According to Table 5, the following conclusions can be obtained:

- (1) The increase in temperature will shorten the initial and final setting times of the slurries.
- (2) The cement slurry has the longest setting time, and the cement–sodium silicate slurry has the shortest setting time.
- (3) There are large differences in the effects of temperature on the three kinds of slurries. The shortening rate of the cement slurry reaches its peak under the condition of 40–60 °C. The effect of temperature on the setting time of the cement–sodium silicate slurry is the smallest. The effect of temperature on the setting time of the RMGS decreases gradually with the increase in temperature.

As the red mud contains calcium chalcopyrite, hard hydrotalcite, acicular ferrite, etc., the amorphous silica-alumina-like substances in the red mud undergo a hydration reaction

to generate a hydration gel under normal conditions, whereas the reactive oxides in the red mud and the CO₂ in the air generate carbonate-based precipitates or colloidal substances, which in turn form calcite; therefore, the RMGS achieves hardening.

In addition, because inert hematite is the main mineral component of red mud, the gelling activity is relatively low, so even under the action of a modifier, the initial setting time is still always maintained at more than 30 min.

On the one hand, in the high-ground-temperature tunnel grouting reinforcement project, the initial setting time of the slurry is required to be above 30 min to ensure the effective diffusion of the slurry in the fissures of the surrounding rock; on the other hand, in order to improve the efficiency of grouting and shorten the construction period, the initial and final setting time of the slurry should not be too long. Therefore, by comparing the setting time characteristics of the three kinds of slurries under high-temperature conditions, it can be inferred that the RMGS is the best material for the grouting and reinforcement project of high geothermal tunnels.

3.3. Compressive Strength

The compressive strength determines the structural bearing capacity of the grouted curtain ring layer. The compressive strength data of the cement slurry, cement–sodium silicate slurry, and RMGS at 20, 40, 60, and 80 °C were obtained through uniaxial compressive strength tests, and the change curves of the three slurries' strengths versus temperatures at different curing ages are shown in Table 6.

Table 6. Table of compressive strength of grouting materials.

Test Materials	Test Temperature/°C	Compressive Strength/MPa			
		1d	3d	7d	14d
Cement Slurry	20	2.79	7.13	12.26	17.51
	40	3.27	8.55	15.06	20.28
	60	4.93	12.05	19.11	26.66
	80	5.02	14.19	23.68	15.71
Cement–Sodium Silicate Slurry	20	3.26	7.29	11.58	14.71
	40	4.38	8.34	15.05	18.20
	60	4.00	7.95	10.24	12.32
	80	3.73	5.83	6.76	6.09
The RMGS	20	3.04	4.65	6.39	7.37
	40	3.30	5.45	6.68	7.36
	60	3.73	6.06	6.82	7.69
	80	3.81	4.21	5.13	4.83

According to Table 6, the following conclusions can be obtained:

- (1) The effect of temperature on the compressive strength of the three slurries has large differences.
- (2) The higher the temperature, the higher the compressive strength of the cement slurry, but at the lower 80 °C 14 d curing age condition, there is a decrease in strength.
- (3) The strength of the cement–sodium silicate slurry reached its peak at 40 °C, and after 40 °C, the strength decreased rapidly; by 80 °C, the strength loss was more than half.
- (4) There are differences in the effect of temperature on the strength of the RMGS under different maintenance age conditions. The increase in temperature at the age of 1 d has an increasing effect on the compressive strength. The compressive strength of the RMGS at the ages of 3 d, 7 d, and 14 d peaked at 60 °C. The strength of the RMGS at 60 °C reached its peak.
- (5) Compared with the cement slurry and cement–sodium silicate slurry, the compressive strength of the RMGS is less discrete and more stable with the change in temperature.

On the one hand, the faster hydration of cement and the higher hydration activity of red mud at high temperatures play a role like that of evapotranspiration, resulting in

higher strength and faster development of the cement, cement–sodium silicate slurry, and RMGS. On the other hand, high temperatures may have several adverse effects on the hydration products, leading to a decrease in strength. At the very beginning of hydration, high temperatures may cause the hydration rate to accelerate, the C-S-H gel to lap in disorder, and the skeleton formed to be less dense. At the time of curing, high temperatures may cause the $\text{Ca}(\text{OH})_2$ generated by the hydration to be dissolved, causing the Ca^{2+} in the C-S-H gel to precipitate out and generating hydroxysilicate calcium stone [30], which may reduce the strength of the crystal skeleton and increase the number of harmful pores, leading to a decrease in strength at a later stage.

Red mud and quartz powder in the RMGS can slow down the hydration and reduce the disordered lap of hydration products. The hydration products of red mud can fill the pores, quartz powder plays the role of aggregate, and the modifier can reduce the dissolution of hydration products. The joint effect of multiple parties enhances the stability of the strength of the RMGS at high temperatures.

3.4. Thermal Conductivity

The thermal conductivity reflects the ability of a material to transfer heat and is the amount of heat transferred through the thermal conductive surface of the material at a unit temperature gradient and per unit time. The thermal conductivity of the cement slurry, cement–sodium silicate slurry, and RMGS was measured at 20, 40, 60, and 80 °C using the protective thermal plate method, and the curves of thermal conductivity of the three types of slurry with temperature are shown in Table 7.

Table 7. Table of thermal conductivity of grouting materials.

Test Materials	Thermal Conductivity/(W/(m·K))			
	20 °C	40 °C	60 °C	80 °C
Cement Slurry	1.175	1.154	1.130	1.102
Cement–Sodium Silicate Slurry	1.142	1.126	1.092	1.052
The RMGS	0.945	0.924	0.898	0.863

As shown in Table 7, the thermal conductivity of the cement slurry is the highest, and the thermal conductivity of the RMGS is the lowest. With the increase in temperature, the thermal conductivity of the cement slurry, cement–sodium silicate slurry, and RMGS showed linear decay. In addition, with the increase in temperature, the decay rate of the thermal conductivity of the three materials increased, the thermal conductivity of the red-mud-based material was the most sensitive to the change in temperature, and the thermal conductivity of the RMGS was further attenuated when the temperature continued to increase.

The reason why the temperature can accelerate the attenuation of thermal conductivity may be that, with the increase in temperature, the hydration reaction rate of cement as well as red mud becomes faster, the hydration products increase, and the thermal conductivity of the hydration products, such as $\text{Ca}(\text{OH})_2$ and C-S-H, is lower than that of the clinker phases, such as C3S, C2S, C3A, etc. [31].

The RMGS exhibits lower thermal conductivity due to more impurities, significantly more hydration reactants than cement, a faster hydration reaction rate, and more hydration products during hydration than cement.

In addition, high temperatures promote the development of pores in cement stone [32], and the effect of porosity on the thermal conductivity of the material is described in the literature [33]. The smaller the volume fraction of the aggregate, the smaller the thermal conductivity of the grouting material, as the aggregate forms a good thermal bridge effect inside the grouting material, and the thermal conductivity of air in the pores is lower than that of the constituents in the solid material. In addition, when the temperature

of the hydration reaction is high, the free water in the material will evaporate, and the dehydration reaction will also lead to a decrease in thermal conductivity. Therefore, with the increase in temperature, the thermal conductivity of the material decreases gradually.

3.5. Specific Heat Capacity

Specific heat capacity refers to the internal energy absorbed or released per unit mass of an object when it changes per unit temperature and reflects the ability of a material to store heat. Using the mixed calorimetry method, the specific heat capacities of the cement slurry, cement–sodium silicate slurry, and RMGS were measured at 20, 40, 60, and 80 °C. The curves of the specific heat capacities of the three types of slurries as a function of temperature are shown in Table 8.

Table 8. Table of specific heat capacity of grouting materials.

Test Materials	Specific Heat Capacity/(J/(kg·K))			
	20 °C	40 °C	60 °C	80 °C
Cement Slurry	883.70	872.42	846.28	826.98
Cement–Sodium Silicate Slurry	804.91	798.59	784.00	774.71
The RMGS	1173.68	1154.67	1121.96	1102.06

As can be seen from Table 8, the specific heat capacities of the cement slurry, cement–sodium silicate slurry, and RMGS all decrease approximately linearly with the increase in temperature. Moreover, the specific heat capacity of the RMGS is the largest, and that of the cement–sodium silicate slurry is the smallest, which is only 70% of that of the RMGS.

The specific heat capacity–temperature relationship equations of the three materials are in line with the linear law of change, with the highest degree of sensitivity in the red-mud-based grouting material and the lowest degree of sensitivity in the cement–water glass bi-liquid slurry.

An analysis of the mechanism of the effect of temperature on the specific heat capacity shows that in the hydration process, the mass of the original solid material does not decrease, and the main factor affecting the specific heat capacity is the content of free water. As the temperature rises, the faster the hydration rate and the more free water consumed. The specific heat capacity of water is $4200 \text{ J} \cdot (\text{kg} \cdot \text{K})^{-1}$, which is higher than the specific heat capacity of the three materials of the nodular body. When the content of free water decreases, the specific heat capacity of the material will also decrease. Therefore, the increase in temperature decreases the specific heat capacity of the material.

An analysis of the reason for the high specific heat capacity of the RMGS shows that the hydration reaction of red mud is the most rapid, and the free water is consumed the fastest, so its specific heat capacity decreases at the fastest rate. However, the hydration reaction of red mud to form the hydration product has a higher specific heat capacity, so the specific heat capacity of the RMGS is significantly higher than the cement and cement–sodium silicate slurries. The higher specific heat capacity makes the curtain arch ring cast with RMGS absorb the heat transferred by the rock body, and its own temperature grows slowly, which plays a role in controlling the tunnel temperature.

4. Discussion

4.1. Microscopic Mechanism

The above tests show that the effect of temperature on the grouting materials is mainly reflected in the rate of the hydration reaction, products, and pore development. To further clarify the microscopic characteristics of the hydration products and pore characteristics of the slurries under different temperatures and raw material conditions, SEM analyses were carried out on the cement slurry and RMGS, as shown in Figure 7.

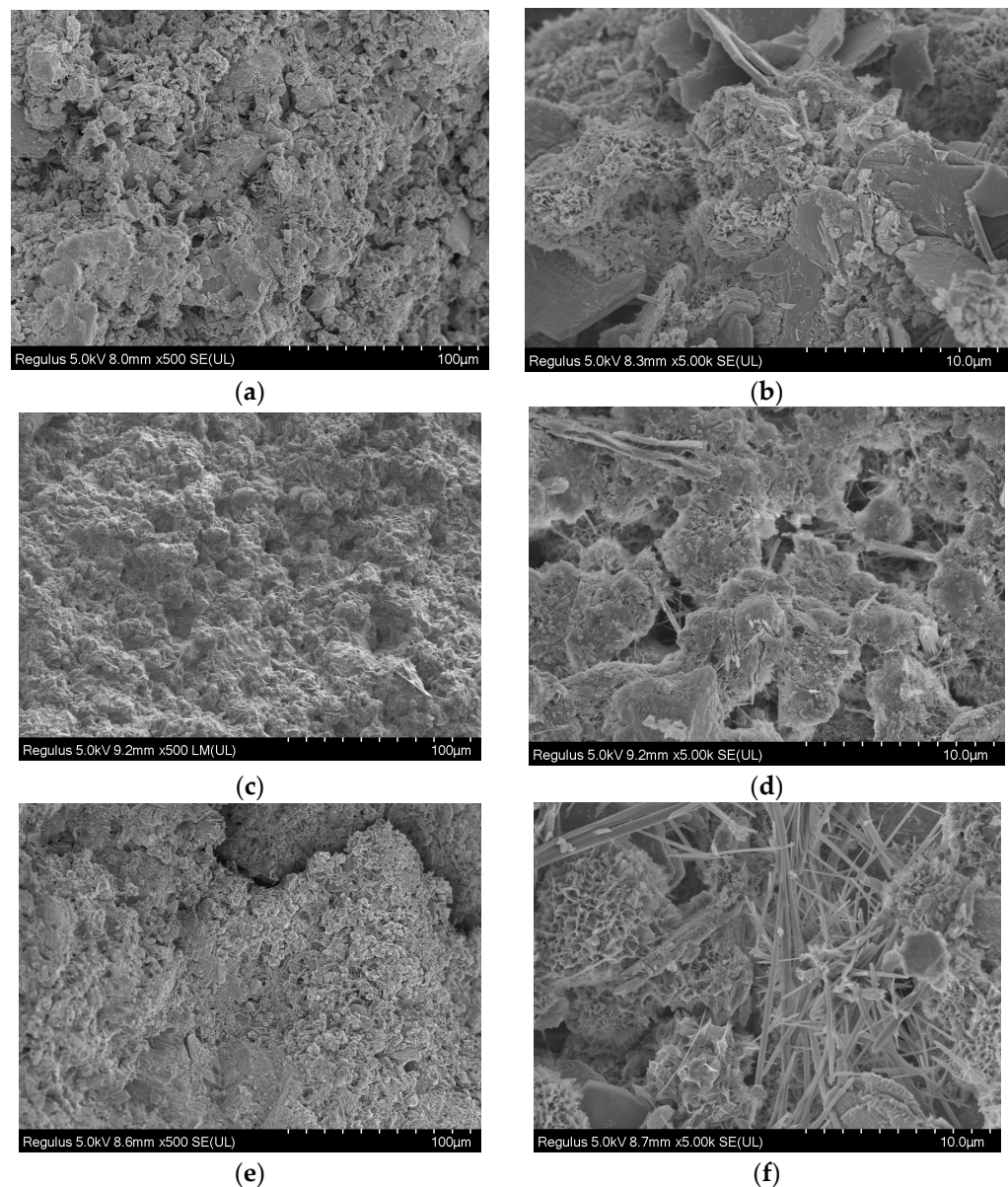


Figure 7. SEM images of each slurry: (a) enlarged by 500 \times , 20 $^{\circ}$ C cement slurry; (b) enlarged by 5000 \times , 20 $^{\circ}$ C cement slurry; (c) enlarged by 500 \times , 20 $^{\circ}$ C RMGS; (d) enlarged by 5000 \times , 20 $^{\circ}$ C RMGS; (e) enlarged by 500 \times , 80 $^{\circ}$ C RMGS; (f) enlarged by 5000 \times , 80 $^{\circ}$ C RMGS.

In Figure 7a,b, the cement slurry contains more pores, and the hydration products are mainly C-A-S-H gel and C-S-H gel. In Figure 7c,d, it can be seen that there are significantly more hydration products of the RMGS than the cement slurry, and its hydration products are mainly C-S-H, C-A-S-H, N-A-S-H, and calcite. The excitation products, due to the low content of calcium in the slurry, mostly contain significantly more N-A-S-H than C-A-S-H and calcite. Under the condition of 80 $^{\circ}$ C (e.g., Figure 7e,f), the increase in temperature accelerated the hydration reaction rate of the grouting material, and the number of hydration products also increased significantly, with C-A-S-H increasing significantly and N-A-S-H gel decreasing gradually. In addition, an obvious needle-like calcite morphology could be found in the slurry.

In addition, the shape of the red mud is more complex, and the particle sizes are different. They are obviously smaller than the cement slurry particles, which makes the voids existing between the particles effectively filled. With the increase in temperature, the red-mud-based grouting material appeared cracked, the rapid development of internal

pores led to a reduction in aggregate volume fraction, and the thermal conductivity also appeared to be attenuated due to the development of pores. The high temperature accelerated the hydration reaction of the red mud, causing the rapid development of viscosity and strength of the grouting material as well as the advancement of the setting time, which also led to a reduction in the specific heat capacity. It also led to the further decomposition of the hydration products and the generation of factors unfavourable to the later strength, which in turn caused the loss of strength of the grouting material in the later stage. In addition, the increase in temperature caused the slurry to undergo thermal expansion, and the combined effect of multiple hydration products resulted in the RMGS generally outperforming the cement slurry and cement–sodium silicate slurry in a high-temperature environment.

4.2. Applications

The three kinds of slurry under high-temperature conditions reflect different properties; therefore, in the actual grouting project, the selection of slurry should be made according to the geological conditions of the site and the characteristics of the grouting materials. Grouting reinforcement of tunnel peripheral rock in different environments has different requirements for grouting materials:

- (1) The surrounding rock is less stable and contains hydrostatic water. This working condition requires the strength of the slurry to be high and for it to effectively reinforce the surrounding rock. The cement slurry reflects the highest compressive strength in the test; therefore, the cement slurry is suitable for peripheral rock grouting reinforcement works with hydrostatic water.
- (2) The peripheral rock fissures are rich in dynamic water, which needs to be grouted to achieve the purpose of water stopping. This kind of working condition requires the slurry to have low viscosity initially, which can flow in the fissure, and after the end of grouting, the viscosity must increase rapidly so that it can be bonded with the surrounding rock to resist the impact of dynamic water. The setting time must be fast to achieve the purpose of stopping water quickly. The cement–sodium silicate double liquid slurry condensation time is short, and viscosity growth is divided into an obvious slow growth stage and a rapid growth stage; therefore, the cement–sodium silicate slurry is suitable for a fissure dynamic water grouting water stopping project.
- (3) The stability of the surrounding rock is poor, containing dynamic water with a fast flow rate and a high temperature of the surrounding rock. This working condition requires the grouting material to meet the strength and resistance to dynamic water scouring ability, and at the same time, it also needs to have the role of heat insulation and temperature control. The RMGS can still maintain the stability of its strength at high temperatures. The slow increase in viscosity in the early stage is needed so that it can spread rapidly in the surrounding rock, and the viscosity of the later stage is rapidly increased, which can prevent the phenomenon of water penetration. Its faster setting time can shorten the working period, in addition to its excellent thermal insulation properties, low thermal conductivity, and high specific heat capacity, so that it can effectively control the temperature of the tunnel interior and improve the working environment. Therefore, the RMGS is suitable for grouting work in high-ground-temperature environments, which requires strength, dynamic water scouring, and heat insulation performance.

5. Conclusions

In this paper, the various properties of an RMGS under different temperatures are investigated, and a cement slurry and cement–sodium silicate slurry are used as control tests to verify the applicability of the RMGS in grouting reinforcement of high geothermal tunnels and to explore the mechanism of the influence of temperature on the performance of the materials. The following conclusions can be obtained:

- (1) The increase in temperature accelerates the viscosity development of the three kinds of grouting materials but does not change the time-varying characteristic law of

viscosity. The increase in temperature accelerates the coagulation of the slurries, but for different slurries, the lifting efficiency shows a large variation. The appropriate increase in temperature improves the compressive strength of the slurries, and when the temperature is too high, the loss of strength is serious.

- (2) The increase in temperature will accelerate the decay of thermal conductivity and the decrease in heat capacity of the three grouting materials.
- (3) The increase in temperature will accelerate the hydration reaction rate of the grouting materials and also lead to the development of internal pores in the materials, thereby affecting the macroscopic performance of the grouting materials.

This research has deepened the understanding of the performance of curtain grouting materials for high-temperature tunnels and studied the applicable conditions of different grouts. The cement slurry is suitable for rock reinforcement in static water conditions. The cement–sodium silicate slurry is ideal for seepage control in fractured rock. The RMGS is well-suited for high-temperature environments, requiring strength, resistance to dynamic water erosion, and thermal insulation. These results can provide an experimental basis for the selection of grouting materials for tunnel curtains in high-temperature mountainous areas.

Author Contributions: Conceptualization, J.N. and Y.Y.; methodology, Y.Y. and J.N.; software, Y.Y.; validation, Y.S. and L.Q.; formal analysis, Y.Y.; investigation, Y.Y.; resources, J.L.; data curation, Y.Y.; writing—original draft preparation, Y.Y.; writing—review and editing, J.L.; visualization, Y.S.; supervision, J.N.; project administration, J.L.; funding acquisition, J.L. and J.N. All authors have read and agreed to the published version of the manuscript.

Funding: This research was supported by the National Natural Science Foundation of China (Grant No. 420510080).

Data Availability Statement: The data used to support the findings of this study are included in the article.

Conflicts of Interest: Author Liangliang Qiu was employed by the company Changsha Hengde Geotechnical Engineering Technology Co., Ltd. The remaining authors declare that the research was conducted in the absence of any commercial or financial relationships that could be construed as a potential conflict of interest.

References

1. Cao, Z.; Li, J.; Ai, Z.; Liu, H.; Zhao, H. Analysis of the effect of uneven high ground temperature on the mechanical properties of tunnel lining. *Railw. Constr. Technol.* **2022**, *355*, 37–42.
2. He, P.; Zhang, G.; Qiang, X.; Qiang, X. Study on the causes and route selection of underground hot water in the Sangzhuling tunnel of the sichuan tibet railway. *J. Railw. Eng.* **2020**, *37*, 10–13+23.
3. Yan, J.; He, C.; Wang, B.; Xu, G.; Wu, F.; Pan, P. Study on the characteristics and mechanism of rock burst in high temperature and high stress tunnels. *J. Railw.* **2020**, *42*, 186–194.
4. Guo, P.; Bu, M.; Zhang, P.; Li, Q.; He, M. Research progress on disaster mechanism and disaster prevention and control of high temperature tunnels. *J. Rock Mech. Eng.* **2023**, *42*, 1561–1581. [[CrossRef](#)]
5. Lin, M.; Zhou, P.; Jiang, Y.; Zhou, F.; Lin, J.; Wang, Z. Numerical investigation on comprehensive control system of cooling and heat insulation for high geothermal tunnel: A case study on the highway tunnel with the highest temperature in China. *Int. J. Therm. Sci.* **2022**, *173*, 107385. [[CrossRef](#)]
6. Qiao, H. Research on cooling and thermal environment characteristics of long single end construction of high altitude temperature tunnel. *J. Undergr. Space Eng.* **2023**, *19*, 632–639.
7. Pu, S.; Wang, H.; Li, M.; Liao, H.; Yao, Z.; Wang, F.; Fang, Y. Research on response measures for high temperature TBM railway tunnel construction. *Railw. Stand. Des.* **2023**, *67*, 116–121+129. [[CrossRef](#)]
8. Kang, F.; Li, Y.; Tang, C.A.; Li, T.; Wang, K. Numerical study on thermal damage behavior and heat insulation protection in a high-temperature tunnel. *Appl. Sci.* **2021**, *11*, 7010. [[CrossRef](#)]
9. Li, Z. Cooling technology and economic research on high temperature tunnel of Yumo railway. *J. Railw. Eng.* **2022**, *39*, 95–99.
10. Yao, W.J.; Lyimo, H.; Pang, J.Y. Evolution regularity of temperature field of active heat insulation roadway considering thermal insulation spraying and grouting: A case study of Zhujidong coal mine, China. *High Temp. Mater. Process.* **2021**, *40*, 151–170. [[CrossRef](#)]

11. Fan, L.; Sun, L.; Yu, Y.; Zhang, J.; Guo, J. The effect of HGM mass fraction and environmental temperature on the performance of cement-based thermal insulation grouting materials. *J. Henan Univ. Technol. (Nat. Sci. Ed.)* **2023**, *42*, 158–164. [[CrossRef](#)]
12. Fan, L.; Sun, L.; Yu, Y.; Zhang, J.; Guo, J. Metakaolin improves the adaptability of cement-based grouting materials in high temperature tunnel engineering. *Mater. Her.* **2022**, *36*, 105–112.
13. Ding, J.; Xi, Y.; Jiang, J.; Wang, H.; Li, X.; Li, H. Changes in cement stone's mechanical and porous permeability characteristics under high and ultra high temperature. *Drill. Complet. Fluids* **2022**, *39*, 754–760.
14. Wang, M.; Hu, Y.; Jiang, C.; Wang, Y.; Liu, D.; Tong, J. Mechanical characteristics of cement-based grouting material in high-geothermal tunnel. *Materials* **2020**, *13*, 1572. [[CrossRef](#)] [[PubMed](#)]
15. Dai, C.; Wang, Y.; Wu, A.; Qi, Y.; Chen, Z. Effect of temperature on the structure of paste slurry at low constant shear rate. *Energy Sources Part A Recovery Util. Environ. Eff.* **2019**, *45*, 2417–2427. [[CrossRef](#)]
16. Duan, L.M.; Zhang, Y.H.; Lai, J.X. Influence of ground temperature on shotcrete-to-rock adhesion in tunnels. *Adv. Mater. Sci. Eng.* **2019**, *2019*, 8709087. [[CrossRef](#)]
17. Cui, S.; Liu, P.; Wang, X.; Cao, Y.; Ye, Y. Experimental study on deformation of concrete for shotcrete use in high geothermal tunnel environments. *Comput. Concr.* **2017**, *19*, 443–449. [[CrossRef](#)]
18. Hu, Y.; Wang, M.; Zhao, D.; Cai, Y.; Tong, J. Heat damage and bond-slip performance of steel arch frame-concrete in high-geothermal tunnels. *Eng. Fail. Anal.* **2021**, *130*, 105514. [[CrossRef](#)]
19. Cui, S.; Liu, P.; Su, J.; Cui, E.; Guo, C.; Zhu, B. Experimental study on mechanical and microstructural properties of cement-based paste for shotcrete use in high temperature geothermal environment. *Constr. Build. Mater.* **2018**, *174*, 603–612. [[CrossRef](#)]
20. Cui, S.; Liu, P.; Cui, E.; Su, J.; Huang, B. Experimental study on mechanical property and pore structure of concrete for shotcrete use in a hot-dry environment of high geothermal tunnels. *Constr. Build. Mater.* **2018**, *173*, 124–135. [[CrossRef](#)]
21. Lv, P.; Xie, Y.; Long, G.; Ma, K.; Zeng, X. The effect of accelerator on the performance of cement paste under high temperature drying. *J. Railw. Sci. Eng.* **2022**, *19*, 2295–2304. [[CrossRef](#)]
22. Chen, P.; Zhang, S.; Yang, H.; Hu, C. Effects of Curing Temperature on Rheological Behaviour and Compressive Strength of Cement Containing GGBFS. *J. Wuhan Univ. Technol.-Mater. Sci. Ed.* **2019**, *34*, 1155–1162. [[CrossRef](#)]
23. Zhang, J.; Wang, C.; Li, S.; Gao, Y.; Zhang, W. Experimental study on engineering characteristics of red mud-based green high-performance grouting material. *J. Rock Mech. Eng.* **2022**, *41* (Suppl. S2), 3339–3352.
24. Liu, Q.; Wang, Q.; Wu, P.; Wang, J.X.; Lv, X.J. Research progress on application of red mud in cementitious materials. *J. Shandong Univ. Sci. Technol. (Nat. Sci. Ed.)* **2022**, *41*, 66–74.
25. GB/175-2007; China Building Materials Academy. Common Portland Cement. Standards Press of China: Beijing, China, 2007.
26. Niu, J.; Wang, B.; Feng, C.; Chen, K. Experimental Research on Viscosity Characteristics of Grouting Slurry in a High Ground Temperature Environment. *Materials* **2020**, *13*, 3221. [[CrossRef](#)] [[PubMed](#)]
27. Gong, H. The influencing factors and error analysis of the thermal conductivity of insulation materials detected by the protective hot plate method. *Bulk Cem.* **2021**, *5*, 120–122+125.
28. Li, S.; Wang, X.; Xia, J.; Shen, D. Test method for specific heat capacity of frozen soil based on the principle of mixed calorimetry. *J. Geotech. Eng.* **2018**, *40*, 1684–1689.
29. Zhang, N.; Wang, M.; Wang, C.; Li, Z.; Ma, C.; Zhang, J.; Peng, S. Preparation and performance study of red mud based grouting reinforcement material. *Mod. Tunn. Technol.* **2023**, *60*, 270–280. [[CrossRef](#)]
30. Wu, Z.Q.; Xie, R.J.; Yang, J.; Ni, X.; Cheng, X. High-temperature mechanical properties and microstructure of high belite cement. *Front. Mater.* **2022**, *9*, 831889.
31. Du, Y.; Ge, Y. A computational model for the thermal conductivity of cement paste. *J. Silic.* **2022**, *50*, 466–472.
32. Ho, L.S.; Nakarai, K.; Eguchi, K.; Ogawa, Y. Difference in strength development between cement-treated sand and mortar with various cement types and curing temperatures. *Materials* **2020**, *13*, 4999. [[CrossRef](#)] [[PubMed](#)]
33. Zhu, D.; Han, Y.; Duan, J.; Shen, L.; Yao, X.; Cao, M. Calculation method for effective thermal conductivity of steel fiber reinforced concrete after high temperature. *Silic. Bull.* **2021**, *40*, 1510–1519. [[CrossRef](#)]

Disclaimer/Publisher's Note: The statements, opinions and data contained in all publications are solely those of the individual author(s) and contributor(s) and not of MDPI and/or the editor(s). MDPI and/or the editor(s) disclaim responsibility for any injury to people or property resulting from any ideas, methods, instructions or products referred to in the content.